Carbohydrate Polymers 229 (2020) 115510

Contents lists available at ScienceDirect

Carbohydrate Polymers

journal homepage: www.elsevier.com/locate/carbpol

Evaluation of nanocellulose interaction with water pollutants using nanocellulose colloidal probes and molecular dynamic simulations

Chuantao Zhu[a], Susanna Monti[b,*], Aji P Mathew[a,*]

[a] Department of Materials and Environmental Chemistry, Stockholm University, 10691 Stockholm, Sweden
[b] CNR-ICCOM – Institute of Chemistry of Organometallic Compounds, via Moruzzi 1, 56124 Pisa, Italy

ARTICLE INFO

Keywords:
Atomic force microscopy
Nanocellulose
Colloidal probe
Force spectroscopy
Molecular dynamics
Water purification

ABSTRACT

Atomic Force Microscope (AFM) probes were successfully functionalized with two types of nanocellulose, namely 2,2,6,6-tetramethylpiperidine-1-oxylradical (TEMPO)-mediated oxidized cellulose nanofibers (TOCNF) and cellulose nanocrystals (CNC) and used to study interfacial interactions of nanocellulose with Cu(II) ions and the Victoria blue B dye in liquid medium. TOCNF modified tip showed higher adhesion force due to adsorption of Cu(II) ions and dye molecules compared to CNC ones. Exploring the adsorption properties through classical reactive molecular dynamics simulations (ReaxFF) at the atomic scale confirmed that the Cu(II) ions promptly migrated and adsorbed onto the nanocelluloses through the co-operative chelating action of carboxyl and hydroxyl species. The adsorbed Cu(II) ions showed the tendency to self-organize by forming nano-clusters of variable size, whereas the dye adopted a flat orientation to maximize its adsorption. The satisfactory agreement between the two techniques suggests that functionalized AFM probes can be successfully used to study nanocellulose surface interactions in dry or aqueous environment.

1. Introduction

In recent years, nanocellulose has been explored extensively as a sustainable and versatile nanomaterial for several applications including water purification. (Ma, Hsiao, & Chu, 2011; Karim, Mathew, Grahn, Mouzon, & Oksman, 2014; Voisin, Bergström, Liu, & Mathew, 2017). The interaction of nanocellulose surface with water pollutants is a complex phenomenon combining different types of interactions, including, for example, van der Waals, electrostatic and hydrogen bonding terms, and various mechanisms such as chelation, entrapments, local reactions, *etc.* Atomic force microscopy (AFM) is one of the most powerful tool to study adsorption in nano and sub-nanoscale through advanced topographical imaging (micro to sub-nanometer resolution) and force measurements (pico-newton sensitivity) in liquid (Ducker, Senden, & Pashley, 1992; Weisenhorn, Hansma, Albrecht, & Quate, 1989) with *ad hoc* customized tips to disclose new insights into the interfacial interactions of different species. (Dufrêne, 2017; Kada, Kienberger, & Hinterdorfer, 2008; Senapati & Lindsay, 2016; Valotteau et al., 2017). AFM tips functionalization by gluing, (Kappl & Butt, 2002) is extensively applied to micro-particles, (Kappl & Butt, 2002) such as silica microspheres that are most widely used as colloidal probes, to investigate surface interactions and forces (*i.e.* the adhesion force against slide surfaces (Herman & Walz, 2015) and living cells (McNamee, Pyo, & Higashitani, 2006), the hydrophobicity of sapphire surfaces (Wada, Yamazaki, Isono, & Ogino, 2017) *etc.* or colloidal probes such as polylactide particles (Nugroho, Pettersson, Odelius, Höglund, & Albertsson, 2013) and microbubbles (Abou-Saleh, Peyman, Critchley, Evans, & Thomson, 2013). In a previous study, we examined the forces at the interface between microspheres of cellulose and Ag(I) in wet conditions *via* force spectroscopy measurements (Zhu, Fang et al., 2015). We found that the irregularity of the cellulose microspheres and their swelling in the aqueous medium affected the accuracy of the measured interactions.

Chemical functionalization route (Barattin & Voyer, 2008; Frisbie, Rozsnyai, Noy, Wrighton, & Lieber, 1994) is adopted to develop colloidal probes using smaller molecules, such as DNA (Möller, Csáki, Köhler, & Fritzsche, 2000), antibodies (Ebner et al., 2007), biomolecules (Kumar et al., 2015; Senapati, Manna, Lindsay, & Zhang, 2013; Wildling et al., 2011), single cell (Beaussart et al., 2014) *etc.*, forming direct chemical bonds to the tip apex (Green, Idowu, & Chan, 2003) and have the purpose of disclosing specific binding events at the molecular level and thus unveil single-molecule inter/intra-molecular interactions (Alessandrini & Facci, 2005; Chtcheglova & Hinterdorfer, 2018; Dufrêne et al., 2011; Mönig et al., 2016). Successful efforts for high resolution AFM imaging were obtained using nanoparticle based colloidal probes too, for example, by placing single CdTe tetrapods on

* Corresponding authors.
E-mail addresses: chuantao.zhu@mmk.su.se (C. Zhu), susanna.monti@cnr.it (S. Monti), aji.mathew@mmk.su.se (A.P. Mathew).

https://doi.org/10.1016/j.carbpol.2019.115510
Received 22 July 2019; Received in revised form 22 September 2019; Accepted 19 October 2019
Available online 22 October 2019

flattened AFM tips (Nobile et al., 2008) and also by attaching to the tips individual carbon nanotubes (Wilson & MacPherson, 2009; Wong, Harper, Lansbury, & Lieber, 1998). One interesting development in this context was the use of a nanofibrillar cellulose coating on the hemispherical polydimethylsiloxane caps as colloidal probe to study the adhesion on biopolymer model surfaces (flat wood) (Gustafsson, Johansson, Wågberg, & Pettersson, 2012). To the best of our knowledge, neither nanocellulose functionalized AFM probes nor force spectroscopy experiments using such probes for characterizing molecular scale interactions are available to date. The aim of the current work is: i) to develop AFM probes functionalized with nanocellulose; ii) to demonstrate their potential to evaluate nanocellulose surface interactions forces with water pollutants, *in situ* in aqueous environment. In the current investigation, we explore the surface interactions of nanoscaled cellulose nanofibers and nanocrystals with copper ions (Shrivastava, 2009) and the Victoria blue B dye (VBB) (Karim et al., 2014), which are two well-known toxic substances that can be found in polluted water.

To support further the experimental characterization, molecular modeling studies at the atomic level are carried out to unveil both the structure and dynamics of TOCNF/CNC, metal ions and dyes. These components are simulated realistically in a complex environment mimicking the experimental setup. The computational models and procedures have been already presented in an earlier work (Zhu, Monti, & Mathew, 2018) where an archetypal hybrid system made of TOCNF fibrils, $CuSO_4$ ions and water, was used to investigate the ability of the matrix to capture metal ions and the tendency to aggregate and form mixed clusters. Here, the model is extended and modified to simulate copper ions and dye molecules adsorption configurations and their dynamics at the substrate interface.

2. Experimental

2.1. Materials

TEMPO-oxidized cellulose nanofibers (TOCNF; carboxyl content 1.0 mmol/g) and cellulose nanocrystal (CNC; carboxyl content 0.5 mmol/g) were prepared at Stockholm University, Sweden following the procedure reported by Isogai et al (Isogai, Saito, & Fukuzumi, 2011) and Mathew et al (Mathew et al., 2014) respectively. Three-component solvent-free epoxy resin Araldite CY212 kit was purchased from Agar Scientific Corporation (U.K.). Copper(II) nitrate hydrate, Victoria blue B, (3-Aminopropyl) triethoxysilane (APTES) were all purchased from Sigma-Aldrich, Germany and used as received. Milli-Q water was used as the dispersion and force measurement medium. ScanAsyst Air probe and SNL-10 probes were purchased from Bruker (USA) which were used for imaging and tip functionalization, separately. All the probes were cleaned in a UV/ozone chamber before modification. Mica sheets (75 × 25 × 0.15 mm) were purchased from TAAB laboratories equipment Ltd, England. The mica was used both for the surface interaction study for the case of Cu(II) and VBB. The AFM image of the mica surface was shown in Fig. 6c.

2.2. Methods

2.2.1. Probe functionalization

Chemical route is adopted for the probe functionalization. The probes were placed in the AFM probe box, and 5 μL APTES was dropped inside the box, which was then kept closed for 30 min.. The surface of probes was homogeneously air coated with APTES vapor during this process. Then, the TOCNF/CNC solution was dropped onto the probe and incubated for 5 min. The probes were rinsed with MQ water at least 3 times to remove free TOCNF/CNC. The probes were investigated by SEM to make sure that they were functionalized with TOCNF/CNC properly. The functionalized probes were used for subsequent force measurements.

2.2.2. Force measurements

The force measurement experiments were performed by a Dimension Icon Atomic Force Microscopy (AFM; Bruker, Nanoscope controller, Santa Barbara, California, USA). The electrochemistry contact mode was applied to take advantage of its quicker and convenient operation when approaching the tip to the same location on the substrate in liquid medium, while the whole force measurements were conducted under contact mode. The fluid probe holder and the protective skirt were used to prevent water leakage or damage to the equipment. The probes were calibrated before functionalization, and the deflection sensitivity values were updated during measurements. The setup parameters were as follows: scan size 500 nm, scan rate 1 Hz, ramp size 300 nm, trigger threshold 0.1 V, number of samples 2048, Z closed loop on. All the force experiments used the same set up parameters. Each of the experiments collected 100–120 force curves and was performed at least 3 times to ensure reproducibility. One set of representative data was selected for discussion and comparison.

2.2.2.1. Metal ions interaction. The functionalized probe (TOCNF or CNC probe) was loaded on the scanner followed by engaging it to the mica surface. MQ water was added, and at least 100 curves were collected. The water was then exchanged for $Cu(NO_3)_2$ solution for Cu (II) adsorption to the TOCNF/CNC probe for 5 min. This exchange was followed by the exchange of the $Cu(NO_3)_2$ solution with MQ water and rinsing of the holder and sample with MQ water adequately to remove free $Cu(NO_3)_2$. MQ water was added to the sample, and at least 100 force curves were collected. Baseline values were used to correct the force curves, and calculations of all the forces were performed. The pull off force values with histograms and normal distribution curves were fitted with Gaussian curves to get the average adhesion force after normalization with corresponding tip radius before and after adsorption of Cu(II). Thus, the surface interaction between Cu(II) and TOCNF/CNC was indirectly estimated based on the adhesion force between the probe and mica in MQ medium with Cu(II) adsorption.

2.2.2.2. Dye interaction. The Victoria blue B solution (50 mg/L) was dropped onto the APTES modified mica surface and rinsed with MQ water to remove free molecules. After drying in air, a layer of Victoria blue B was homogeneously coated on mica and used for the force measurement between the TOCNF/CNC and Victoria blue B. 100–120 force curves were first collected between the TOCNF/CNC probe and mica and then between the TOCNF/CNC probe and Victoria blue B, both in MQ water medium. The data were analyzed in the same way as with the indirect method.

2.3. Characterizations

2.3.1. Atomic Force Microscopy (AFM)

ScanAsyst Air probe (spring constant = 0.4 N/m) under ScanAsyst mode was applied for nanocellulose, mica and Victoria Blue B surface morphology imaging measurements. SNL-10 probes and the number B cantilever with a spring constant of k = 0.12 ± 0.02 N/m (determined by the thermal tune method (Kim, Choi, Kim, & Park, 2010) using the built-in option in AFM software Nanoscope 9.1) was chosen and calibrated before tip functionalization and force measurements. All cantilevers were cleaned in a UV/ozone chamber for 20 min before modification. The collected data were processed with the NanoScope Analysis 1.5 software (Bruker).

2.3.2. Scanning electron microscopy – energy dispersive X-ray spectroscopy (SEM-EDS)

The AFM probes with and without functionalization and the functionalized probes after force measurements were observed using scanning electron microscopy on a JEOL JSM-7000 F microscope (Japan). The samples were placed on conductive carbon tape without any coating to avoid damaging the nanocellulose functionalized on the

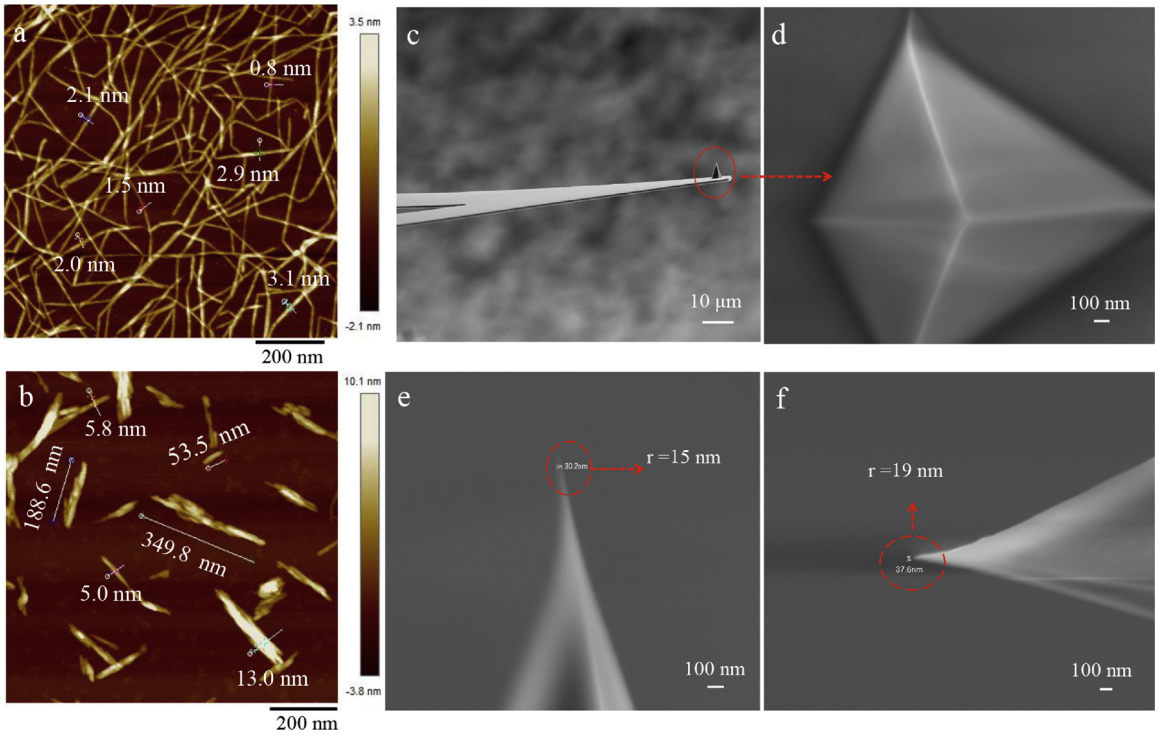

Fig. 1. Morphology of the nanocellulose and AFM probe. AFM images of TOCNF (a,) and CNC (b); SEM images of the clean AFM probe after calibration, side view of the cantilever with tip (c), top view of the tip (d) and the corresponding side view of the tip after calibration showing tip radius of 15 nm (e), and the tip after functionalized with CNC showing the tip radius of 19 nm measured by SEM (f).

probes. Images were taken at 5 kV and 10 mm working distance was used for the EDS measurements. Spot and map profiles showed the elemental distribution on the samples surface. The functionalized probes used for force measurements were investigated only after force measurements to prevent any damage to the nanocellulose that may have affected the force measurements. All AFM probes were imaged by SEM after the experiments and inspected for defects, cracks, or evidence of contamination.

2.4. Molecular modeling

2.4.1. Model building

The TOCNF/CNC structure is made of sixteen chains, containing sixteen glucosyl residues each, arranged as a parallelepiped rod. Only one facet, chosen to reproduce an infinite substrate, is functionalized (TOCNF) with carboxyl groups and the infinite slab is obtained by replicating the system in x and y directions (periodic boundary conditions – see Fig. S2). The size of the fibril is around 84 × 25 × 25 Å3. Considering the type of support, we believe that the size we have chosen is sufficient to simulate the variability of the environment and, at the same time, to represent reasonably the experimental observations at an affordable computational cost. Indeed, according to the experimental characterization the size of the cellulose nanofibers is widely distributed (50–1000 Å) and the average diameter is around 380 Å. This, in our modeling case, is equivalent to an infinite system.

The initial conformation of VBB was built by mutation of the ISIPEH (CID) structure downloaded from the Cambridge Structural (Groom, Bruno, Lightfoot, & Ward, 2016) and optimized at the M062X/6-311 + G** level. Before creating the complete configurations, the validity of the cellulose nano fibril models, namely CNC and TOCNF, and their behaviour in water solution were checked by means of short atomistic molecular dynamics (MD) simulations based on a ReaxFF force field appropriately parametrized to describe these kinds of systems (see Ref.(Mathew et al., 2014) and references therein). Essentially, these checks were pre-equilibrations of the systems in the NPT ensemble, at 300 K and 1 atm, to prepare the supports for the subsequent simulations in crowded environments. The equilibrated models were then used as initial configurations of the substrates in the simulations with copper ions, dyes, counterions and waters.

2.4.2. Molecular dynamics simulations

Four multicomponent configurations were prepared and simulated for hundreds of picoseconds until they reached their final equilibration. They consist of one of the two supports (CNC or TOCNF), five molecules of VBB with its respective Cl^- counterions, or 32 Cu(II) ions with their respective NO_3^- counterions and around two thousand water molecules. The most crowded scenario contained about ten thousand atoms. No restraints were introduced in the systems and reactivity was always considered as the protonation and deprotonation of the carboxyl moieties and other possible reactions involving, for example, the hydroxyl groups in response to the surrounding environment. All the MD simulations were performed with the Amsterdam Density Functional (ADF)/ReaxFF (Baerends et al., 2016). The systems were first equilibrated in the NVT ensemble and then at constant pressure and temperature (T = 300 K, P = 1 atm) for about 300 ps. Subsequently, the production dynamics were performed in the NVT ensemble for about 1 ns and system structures were collected every 0.1 ps. Temperature and pressure were controlled through the Berendsen's thermostat and barostat (Berendsen, Postma, Van Gunsteren, Dinola, & Haak, 1984) with relaxation constants of 0.1 ps and the time step was set to 0.25 fs. Considering that we were interested in disclosing the characteristic adsorption of the metal ions and dye on each model substrate, and that both dye molecules and metal ions were already near the supports at the beginning of the simulations, the simulated production time span was substantial to reach the final settlement. Thus, the analysis of the sampled data was focused on the last portions of the trajectories, which were obtained from several simulations with different starting positions of Cu(II) ions and dye molecules in relation to the substrates (at a distance of about 8 Å). The final analysis collects all the data of the MD runs and tries to depict and predict the various tendencies of adsorption

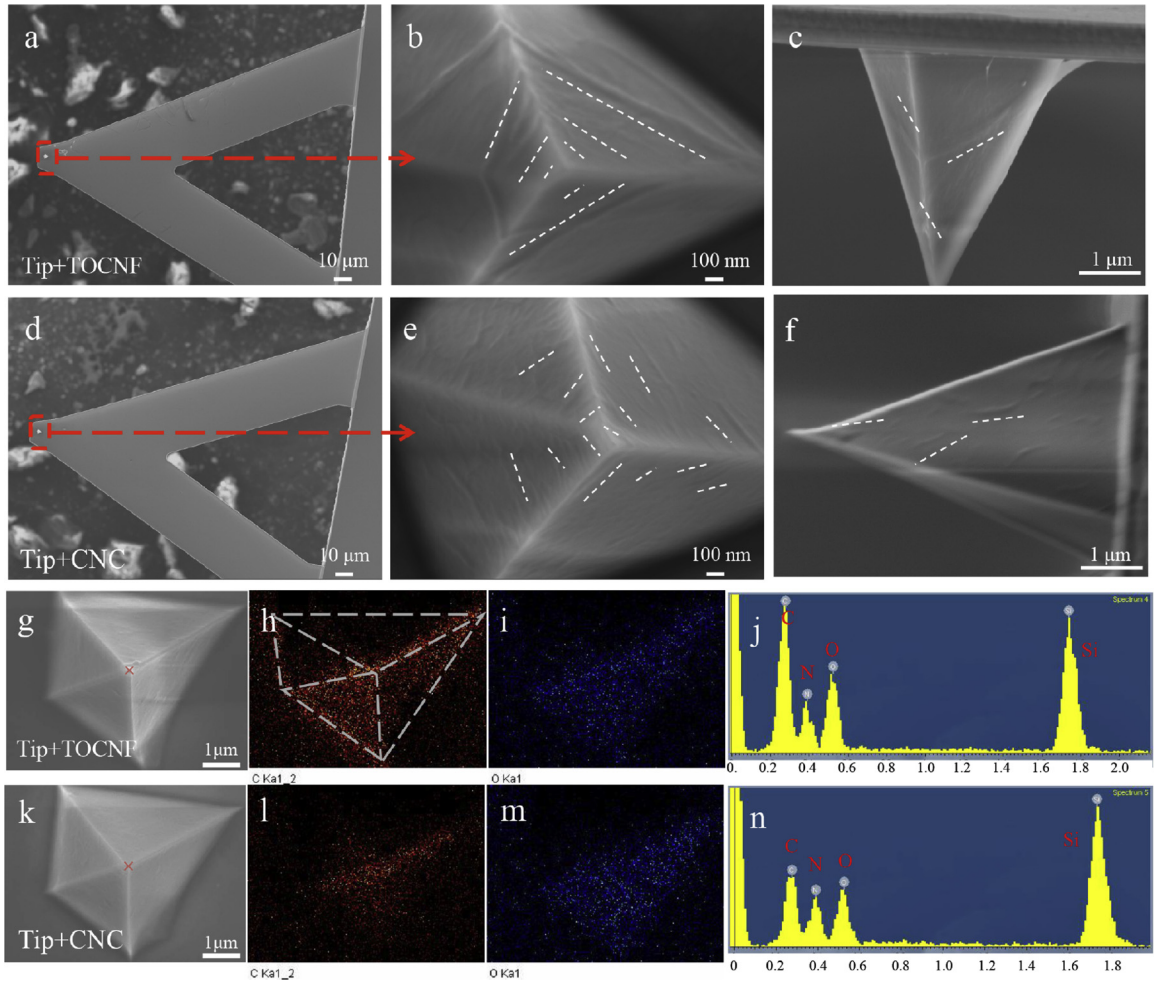

Fig. 2. AFM probes modified by chemical functionalization method using APTES as cross linker. AFM probes functionalized with TOCNF (top view: a and b, side view: c) and CNC (top view: d and e, side view: f). The red cross (g and k) shows the tip apex and the corresponding EDS spectrum is displayed in j and n for TOCNF and CNC, respectively. (h, i) and (l, m) represent the carbon and oxygen EDS maps on the TOCNF and CNC tips, respectively. The white broken lines indicate the location of the visible nanofibers attached on the tip surface. (For interpretation of the references to colour in this figure legend, the reader is referred to the web version of this article).

on the supports in connection with experiments.

The examined descriptors are mainly atom-atom radial distribution functions (RDFs), spatial distribution functions (SDFs) and hydrogen bonds. However, visual inspection of the trajectories was fundamental to understand the adsorption scenarios and evidence the different adsorption characteristics.

3. Results and discussion

3.1. Cellulose nanofiber and nanocrystal

The cellulose nanofibers (TOCNF, Fig. 1a) and nanocrystals (CNC, Fig. 1b) decorated with carboxyl functional groups, displayed in Fig. 1, were selected as representative species for tip functionalization. The carboxyl group content in TOCNF (1.0 mmol/g) is twice that observed in CNC (0.5 mmol/g). Beside the presence of carboxyl groups, which are responsible for the greater adsorption capacity of TOCNF in relation to CNC, major distinctions are found in the structural organization: TOCNF are in the form of fibrils, composed of both ordered and disordered regions, whereas CNC are short and rod like chains, containing only ordered structures (Nobile et al., 2008).

The nanocellulose diameters, determined from the height images (to avoid the tip broadening effect), were in the range 1 to 3 nm for the long TOCNF filaments (hundreds of nm to μm) and approximately 5 nm for the shorter CNC segments (less than 300 nm). This is clearly visible in Fig. 1a-b where the diameters of a few representative TOCNF and CNC samples are marked. The broad range of values appearing there, testifies the well-known size distribution scenarios that are essentially due to the processing procedures and sample preparation routes (Isogai et al., 2011; Mathew et al., 2014).

The research was conducted focusing on two major stages: i) chemical functionalization methods to modify the AFM tips with the above-mentioned cellulose nanofiber and cellulose nanocrystal, ii) investigation of the interactions between the AFM probes and metal ions/dyes.

3.2. Functionalization of AFM tips

Considering that surface interaction measurements require a sharp AFM tip with a nanoscale apex, we have chosen a probe (SNL-10, Bruker) with theoretical tip radius in a range between 2 and 12 nm, which can be considered an ideal option. However, the tips are quite easily worn and could become less sharp after scanning with force set point even in nN range. Furthermore, the spring constant of the probes varies among different batches. Therefore, we first calibrated the cantilevers to obtain a proper spring constant, and then examined them by SEM (top and side view in Fig. 1c-e) to check the quality of the tip apex. After calibration, the tip radius was around 15 nm as shown in Fig. 1e. The parameters for each tip were collected and used for force

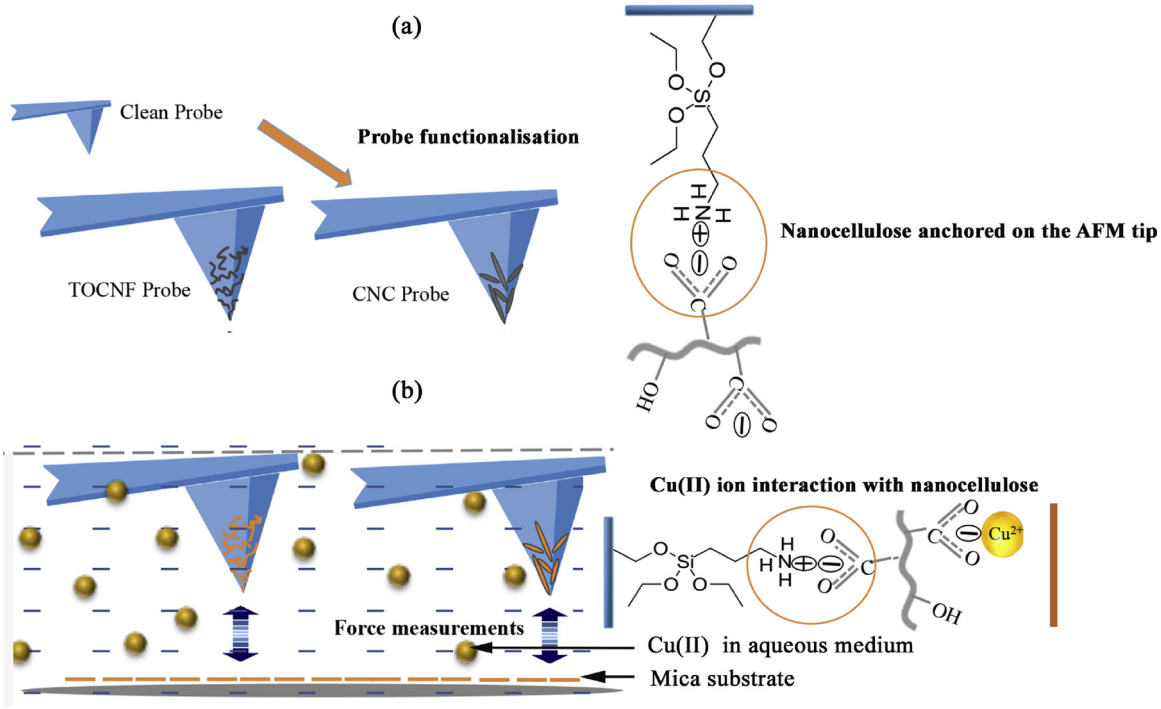

Fig. 3. Scheme of the probe functionalization and force measurement by indirect method. (a) AFM tip functionalization with TOCNF and CNC anchored using APTES. (b) The force measurements using TOCNF/CNC probes on the mica substrates in a solution of Cu(II); The adsorption of Cu(II) by TOCNF/CNC-functionalized tips through electrostatic interaction. The colour change of nanocellulose in b indicates that the Cu(II) ions were adsorbed on the surface of TOCNF/CNC.

measurements by the built-in software - Nanoscope Analysis 1.5 (Bruker, USA). The pull off forces were recorded and normalized by the tip radius for the discussion of the adhesion force.

3.2.1. Chemical functionalization of probes

[(3-aminopropyl) triethoxysilane] (APTES) is being routinely used for the chemical modification of the AFM tips. The modification is made in the gas phase by silanization where only one ethoxy group reacts with Si_3N_4 on the tip, whereas the other two are connected to the adjacent -O—Si—O— groups and extend the -NH_2 moieties far from the surface (Chtcheglova & Hinterdorfer, 2018). On the basis of the characteristics of the surrounding environment, three types of reactions between the tip anchored APTES and nanocellulose groups may be expected: i) in weak acidic solution, the —O—Si—O— chain could form Si—OH groups and bind the —OHs of nanocellulose ii) the Si—OH groups could react with —COOH of nanocellulose iii) the —NH_2 groups could form hydrogen bonds with —COOH groups of nanocellulose. These kinds of interactions can be all present in different proportions depending on local conditions.

Fig. 2 displays the top and side views of both probes and tips after functionalization with TOCNF/CNC. Fig. 2 shows the tip apex covered with nanoscaled TOCNF and CNC which is expected to facilitate the force measurements at the nanoscale. The tip apex with a diameter of around 19 nm after functionalized with CNC is shown in Fig. 1f.

SEM in combination with Energy Dispersive X-Ray Spectroscopy (SEM-EDS) was used to determine qualitatively/semi-quantitatively the elemental composition of the tip apex and to prove its functionalization with nanocellulose. Fig. S1a-f show the SEM-EDS spectrum, the maps of the clean tip and the maps of the tip functionalized with APTES, while Fig. 2g-n exhibit the data for the tip functionalized with TOCNF and CNC. As expected, inspection of the EDS spectrum of the clean tip (Fig. S1b) reveals that mainly silicon and nitrogen were present, being the components of the used Si_3N_4 tip. The occurrence of oxygen is due to the rapid decomposition and oxidation at room temperature on exposure of the silicon nitride surface to air (Fig. S1b). The spectrum clearly shows the increased intensity of carbon and oxygen after functionalization with nanocellulose (Fig. 2j and n), in comparison with the unmodified case (Fig. S1b and S1f), suggesting that nanocellulose was attached on the tip apex (red cross). Indeed, the corresponding carbon and oxygen EDS maps resulted in dense and homogeneous distributions of these two elements (Fig. 2h–i and L-m) larger than those obtained for the tip coated with APTES, (Fig. S1d-e). Thus, both SEM images and EDS spectra indicate that the functionalization of the tips with nanocellulose chains had taken place.

It is worth mentioning that from an operational point of view the chemical functionalization procedure was simpler and more reproducible than the gluing method we have attempted (data not shown) where the constant presence of impurities affected frequently the quality of the results (Wildling et al., 2011). With the chemical method the tip contamination was almost absent and the potential damage of the tip apex could be avoided because the technique did not require tip-substrate contacts. Furthermore, the unbound nanocellulose could be removed from the surface by rinsing with MQ water after functionalization, leaving possibly a monolayer of TOCNF/CNC on the tip surface as evidenced by the measure of the tip radius after modification. Taking into account all these positive results, the probe modification by chemical functionalization is appropriate for investigating surface interaction/adhesion and performing force measurements.

3.3. Surface interaction studies

Before starting the discussion, it is worth pointing out that in the case of copper ions, the interaction between nanocellulose and the substrate was evaluated indirectly by measuring the changes induced on the modified tips by the adsorption of copper ions(indirect method), whereas in the case of the dye (Victoria blue B) the interaction between nanocellulose and dye could be directly detected because of the larger size of the dye, its self-assembly ability and its anchoring to the substrate(direct method).

The interactions between the nanocellulose and amine head groups from APTES on the Si_3N_4 tip surface stabilize the probe as shown by similar studies found in literature (Corno et al., 2015; Dhamodharan &

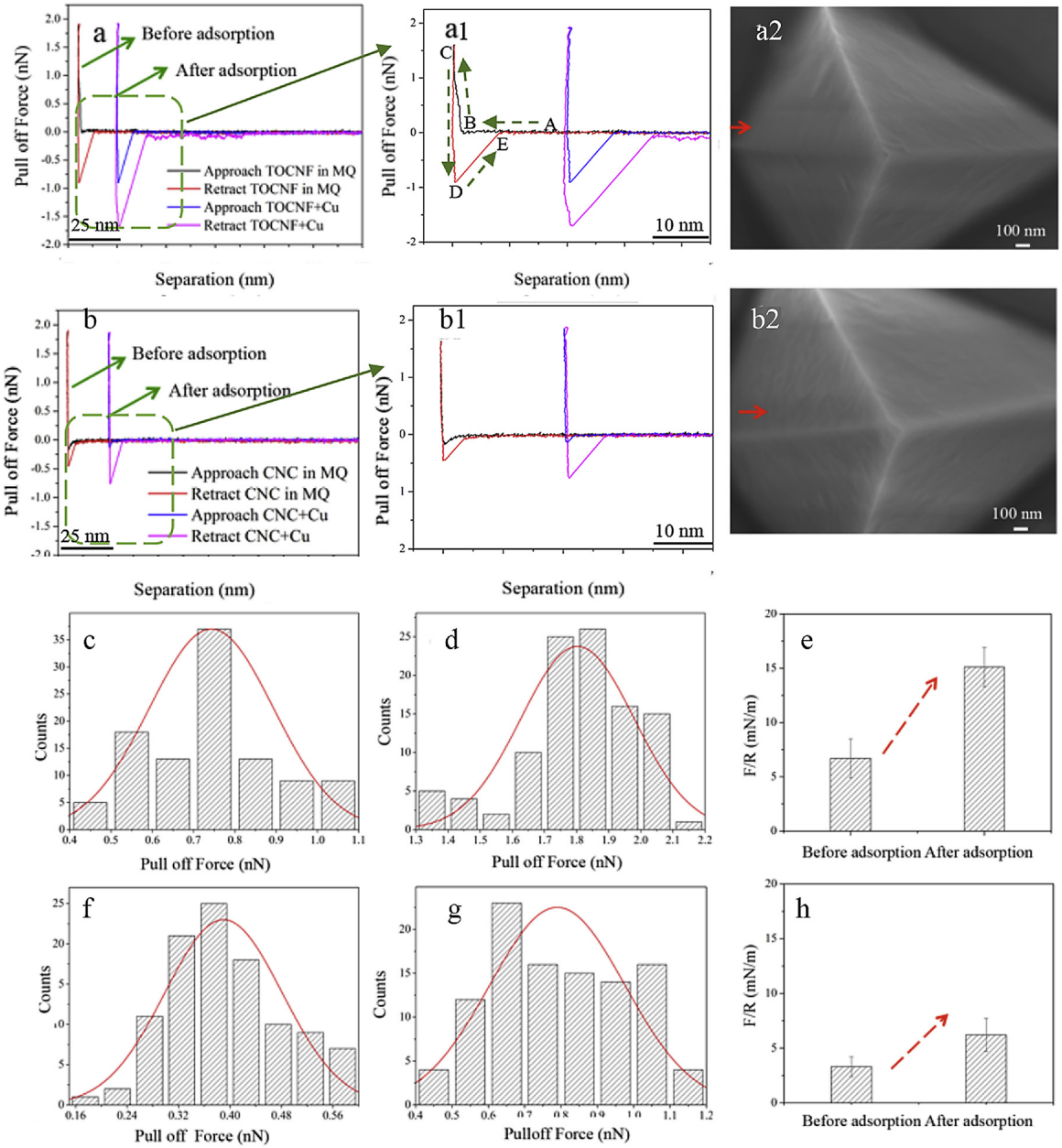

Fig. 4. Force spectroscopy data of the interaction of the metal ions with the nanocellulose functionalised probes and SEM images of the probes after force measurements. The representative force curves for the interaction between TOCNF probe and mica surface (a), zoom of the rectangular area (a1) and the representative force curves between the CNC probe and mica surface (b), the zoom of the rectangular area (b1) are given. SEM images of the tip from TOCNF (a2) and CNC probes (b2) after force measurements (top view) are shown. The histogram of the distribution of pull off forces for TOCNF probes before (c) and after (d) Cu(II) adsorption and the corresponding normalized average adhesion force value (e);, the histogram of the distribution of pull off forces for CNC probes before (f) and after (g) Cu(II) adsorption and the corresponding normalized average adhesion force (h).

McCarthy, 1999; Wildling et al., 2011). Essentially, TOCNF/CNC engage their hydroxyls and/or carboxyl groups in hydrogen bonding interactions/salt bridges with the amine moieties of APTES. It was considered that tip modification involved only a small fraction of the functional groups present on the TOCNF/CNC surface and thus the groups sterically available after the initial functionalization process (see Fig. 3a) could be reached by other “complementary” species dispersed in the surrounding environment, which actively play the key role of surface interaction towards the water pollutants.

3.3.1. Surface interactions between nanocellulose and copper(II)

The Cu(II) interaction with both TOCNF and CNC probes was experimental designed based Schematic representation in Fig. 3b where the changes in interaction between nanocellulose functionalized probe and a mica surface is measured in aqueous medium without and with Cu(II) ions. The representative force curves are shown in Fig. 4a, a1, b, b1 for the TOCNF and CNC cases, separately. To further evaluate the stability of the functionalization, a cross-check of the TOCNF/CNC probes was carried out by using SEM after force measurements. It was found that the TOCNF/CNC particles remained on tip and tip apex (Fig. 4a2 and b2). This confirms that the nanocellulose is anchored strongly on the AFM probe through APTES and the interaction with mica surface or the metal ions in the water do not detach them during measurement.

As was shown in Fig. 4a1, the TOCNF probe cantilever approaches the mica surface from point A and contacts the surface at point B with a

repulsive force until it reaches point C. Then the tip starts to retract from the surface but still remains in contact with the surface due to attractive forces until point D, which shows the maximum pull off force. Finally, the tip leaves the surface and loses the contact at point E. The pull off forces were collected and converted to adhesion forces by normalizing them with respect to the tip radius (Fig. 4a2 and b2).

The TOCNF probe interacting with mica in the aqueous medium (Fig. 4a and a1) shows low repulsion forces at distances around 2 nm, which are much shorter than the ones considered in an earlier study at the micro scale (separation distance around 100 nm) (Zhu, Dobryden et al., 2015) and could be ascribed to the presence of the week double-layer repulsion (higher than the Van der Walls attraction) arising from negative charges on the mica surfaces and the TOCNF chains on the probe. The retraction curve was very clear and sharp, showing an average adhesion force around 6.7 mN/m (Fig. 4i). We could speculate that the main interactions of TOCNF and CNC with the mineral surface are between the oxygens/K^+ ions on mica and the hydroxyl/carboxyl groups of the TOCNF/CNC chains (Das & Bhattacharjee, 2005; Pezron, Pezron, Claesson, & Malmsten, 1991), leading to the adhesion force.

In the presence of Cu(II) ions, no repulsive forces were measured during the approach path except for a large snap-in at a separation of about 7 nm (Fig. 4a), indicating an attractive force of approximately 1 nN, which is the combination of electrostatic attraction and Van der Walls attraction. The pull off forces mainly fall in the range of 1–2 nN, which is much lower compared with the forces (2–6 nN) measured by us using cellulose microsphere probes in a similar experimental setup (Zhu, Dobryden et al., 2015). After normalization, the adhesion force between the nanocellulose probe and the mica surface observed after adsorption of Cu(II) (Fig. 3) increased from 7.3 to 15.1 mN/m (Fig. 4e). This difference could be mainly ascribed to electrostatic interactions between the positively charged Cu(II) and the negatively charged surface of mica (Sides, Faruqui, & Gellman, 2009). It could be inferred that after adding Cu(II) to the system, the copper ions quickly migrate onto the nanocellulose probe (Fig. 3) and re-modulated the total charge of TOCNF on the tip (Zhu, Liu, & Mathew, 2017). It is also important to consider that, mica (muscovite) with K^+ ions (Monti, Alderighi, Duce, Solaro, & Tiné, 2009) can strongly interact with Cu(II) ions in mild acidic water solutions through various mechanisms, such as outer- and inner-sphere complexation, ion exchange, precipitation, that could also occur in combination (Farquhar, Vaughan, Hughes, Charnock, & England, 1997). Moreover, copper ions can induce the release of K^+ ions from mica in solution and also replace them. The measured retraction curve was close to the baseline at zero force, and showed a low noise levels after pull off. This suggests that the Cu(II) adsorption forming Cu(II) clusters on the surface of TOCNF (Zhu et al., 2018) led to a softer tip apex and a weaker elastic force between the interacting chains.

Similar interactions were observed for the CNC system and the representative force curves were displayed in Fig. 4b. A repulsive phenomenon is observed during approach in the TOCNF case (Fig. 4a1), whereas a snap in was observed in the approaching curve in the case of CNC (Fig. 4b1). As mentioned, the carboxyl group content in TOCNF is twice as much as that present in the CNC. Thus, the double layer repulsive force is lower in the CNC case, whereby the van der Walls attraction dominates the interaction, leading to the jump to contact effect. It is apparent that the normalized adhesion force between the CNC probe and the mica surface increases from 3.3 to 6.2 mN/m due to the adsorption of Cu(II) (Fig. 4h). This is attributed to the intermolecular interactions between CNC with captured Cu(II) ions and the negatively charged mica surface. Instead, in the case of CNC, which contained a lower number of carboxyl groups, the adhesion strength was lower. No significant noise could be detected from the retract curve indicating that the adsorption of Cu(II) and the Cu(II) clusters was lower than that observed in the TOCNF case. Owing to the sharp tip apex even after modification with nanocellulose, the noise level was almost avoided in all the subsequent measurements. This was a significant improvement as the noise is usually more pronounced during interaction with micro sized, round particles (Zhu, Dobryden et al., 2015) and some large molecule-functionalized probes (Kumar et al., 2015; Möller et al., 2000). This is because microparticles have a larger contact area, which makes pull off more complex and delayed than a sharp tip; furthermore, the micro sized cellulose particles are more prone to swelling in the liquid medium and change of stiffness. This induces a deformation when the particles are in contact with the surface, leads to longer separations and produces considerable noise during pulling off from the surface.

3.3.2. Molecular dynamics simulations

The molecular modeling description at the atomic level was very helpful and capable of giving a more complete view of the characteristic features of the nanocellulose materials responsible for the capturing process of ions/dyes, which is usually due to the cooperation of the carboxyl and hydroxyl groups of the biopolymers' chains.

A first interesting data emerging from the simulations, was the confirmation of the negatively charge character of the TOCNF/CNC matrices, obtained through the evaluation of the individual atomic charges of the interfaces and their sums in the final average configurations. It was found that in response to the environment, *i.e.* to the adsorption of metal ions and dyes, all the matrices were negatively charged with TOCNF three times more negative than CNC due to the presence of the carboxyl groups. In addition, all the models were well solvated by the surrounded water and showed the tendency to inflate or swell. This was confirmed by the increasing root mean squared deviations of the carbon atoms of the chains in relation to the more compact arrangements of the starting configurations. Indeed, the average final values were stabilized in 8–11 Å range. Regarding TOCNF/CNC interactions with the Cu(II) ions, it was observed that cation adsorption took place effectively, as confirmed by the sharp peaks at short distances visible in all the plots of the radial distribution functions (RDFs) between the Cu(II) ions and the oxygen atoms of the supports (Fig. 5). Although at the beginning of the simulations all the metal ions were wandering in solution, relatively far from the cellulose interface, during the simulations they had the tendency to migrate toward the substrates and, at the end of the simulations, they were found in contact with the nanocellulose chains, accommodated on top of the surface and strongly connected to the carboxyl groups of TOCNF or entrapped by the concerted action of the different oxygen species of the CNC chains (Fig. 5). Essentially, they were stably adsorbed and could also be organized in small clusters of various sizes and shapes depending on their relative locations. Further evidence was obtained by inspecting the spatial distribution functions that testified the permanence of the ions in their final locations.

3.3.3. Surface interactions between nanocellulose and Victoria blue B

Moving to the investigation of the adsorption of the VBB dye on TOCNF and CNC, we performed a series of surface interaction studies that consisted in measuring directly the forces between nanocellulose and the dye.

The height images of the modified VBB-mica surfaces showed that the VBB molecules were aggregated in very small nanoparticles and were anchored onto mica (Fig. 6(d)). After surface modification, the average surface roughness increased from 0.11 to 0.18 nm (Fig. 6(d)), indicating that a layer of VBB was anchored on the mica substrate. This resulted in a relatively homogenous positively charged surface for force measurements. In parallel, MD simulations, in the complex environment described in the Materials section, were carried out to reproduce the dynamics of the dye in relation to binding modes on the substrate as well as the nanocellulose for comparison with the experiments. Interestingly, it was found that the dye could self-assemble and form stacked and T-shaped complexes, both in solution and when in contact with the support. The model also suggested that the dye aggregates contain a great variety of mixed stacked-T-shaped complexes with a positively

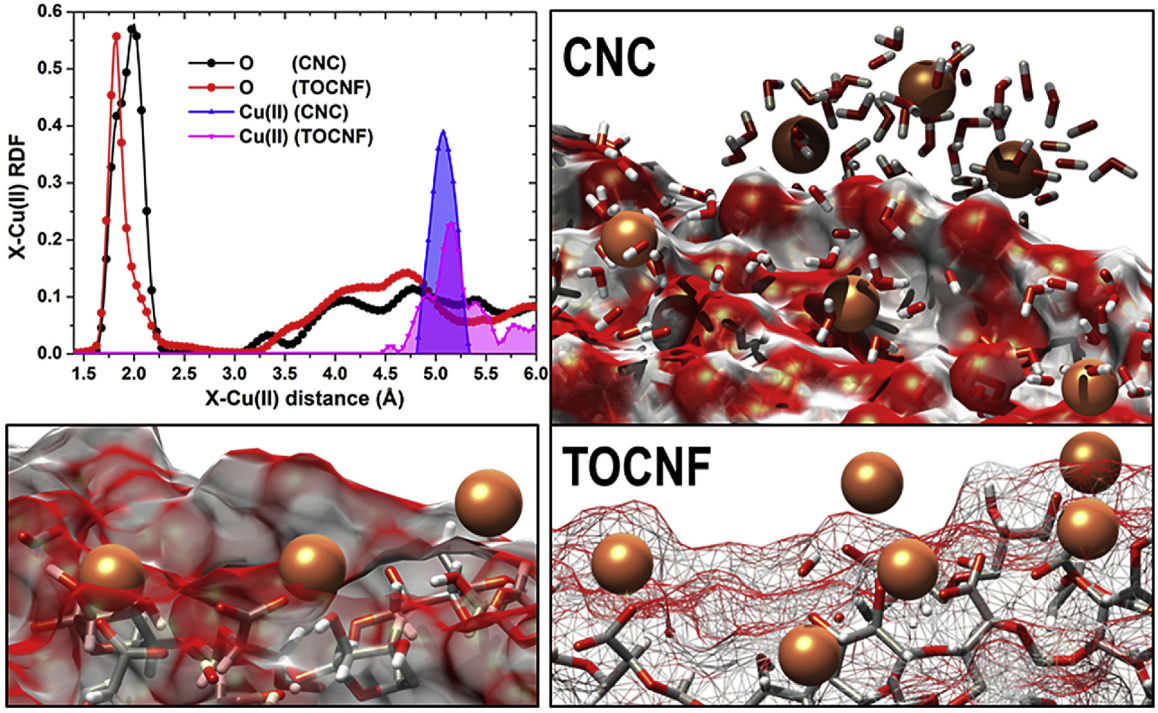

Fig. 5. Top Left. Normalized atom-atom Radial Distribution Functions of the adsorption of the Cu(II) ions on CNC and TOCNF. Cu ions are represented by orange spheres; oxygen, hydrogen and carbon atoms are rendered through red, white and grey sticks, respectively. CNC and TOCNF (bottom left and right) supports are represented by means of solvent accessible surfaces (solid or mesh contours) colored according to the atom type. All the oxygen atoms of the supports have been considered and also Cu(II) - Cu(II) RDFs have been calculated to have an idea of the ion clustering tendency. This is apparent in the case of TOCNF where low peaks at shorter distances are present. Right hand side: A few arrangements of the adsorbed Cu(II) ions are shown for the CNC (top) and TOCNF (Bottom: left and right) supports. A few water molecules are displayed to underline the fact that the ions could be partially solvated. In the case of TOCNF they can be entrapped by the concerted action of hydroxyl and carboxyl groups. Water molecules, counterions and portions of CNC and TOCNF substrate have been undisplayed for clarity. (For interpretation of the references to colour in this figure legend, the reader is referred to the web version of this article).

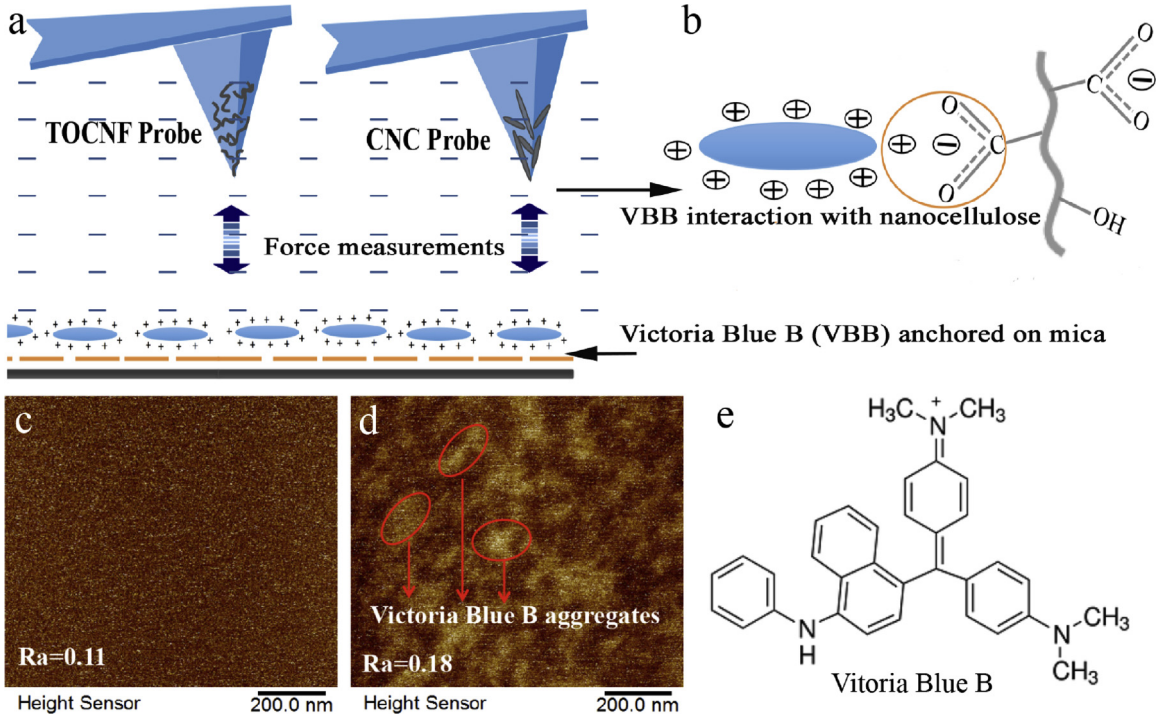

Fig. 6. Scheme of the force measurement by direct method (a) showing Victoria Blue B(VBB) anchored on the substrate (mica) surface and the force measurement between TOCNF and CNC modified probes and VBB on mica surface in MQ water. The interaction between TOCNF/ CNC and VBB is represented in the image (b). (c) and (d) are the AFM images of mica and dye modified surface on mica, respectively. Ra stands for average surface roughness. e) Molecular structure of Victoria Blue B in water. (For interpretation of the references to colour in this figure legend, the reader is referred to the web version of this article).

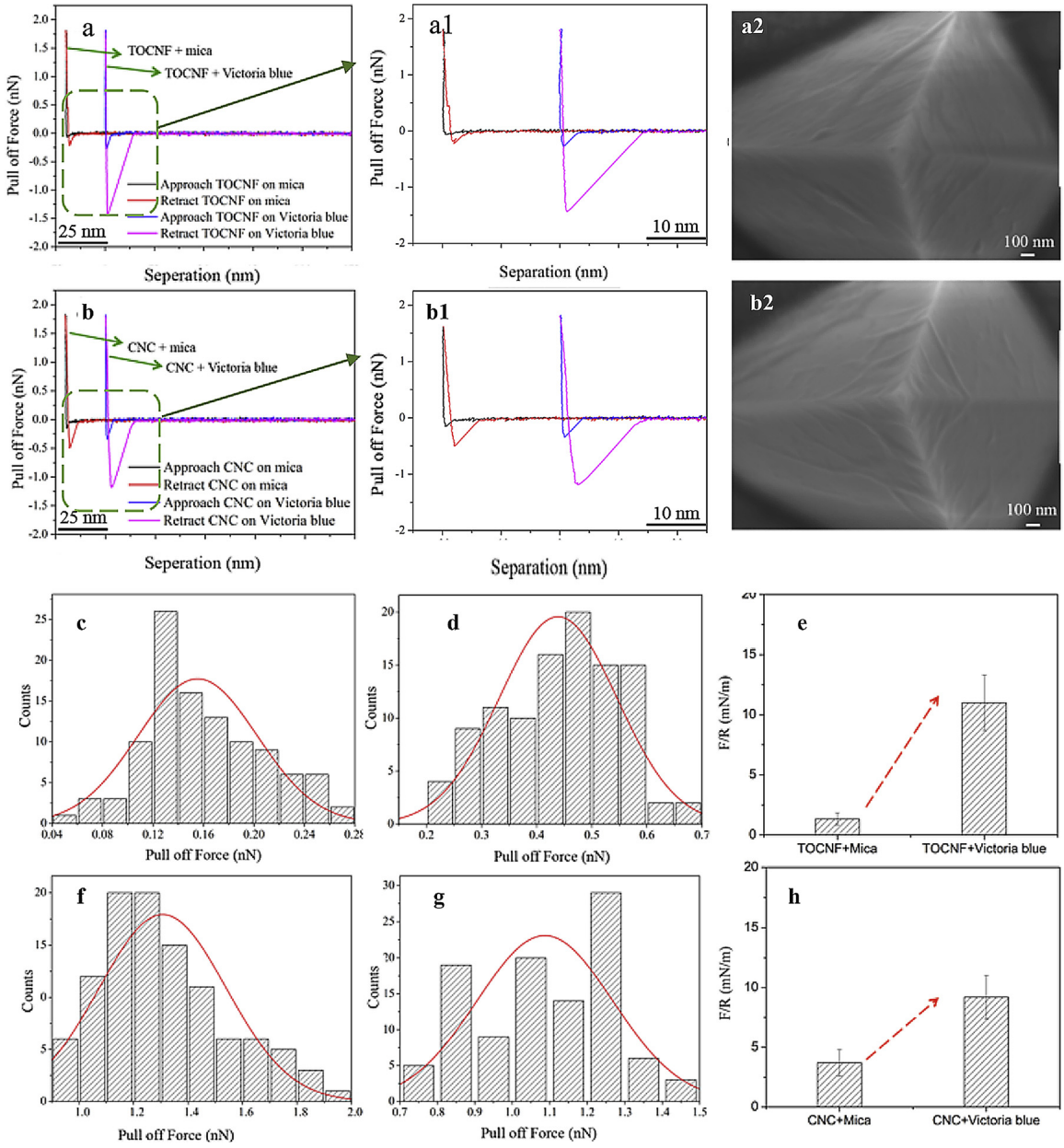

Fig. 7. Force spectroscopy of the interaction of the dye with the nanocelluose functionalised probes and SEM images of the probes after force measurements. Representative force curves between TOCNF probe with clean mica surface and VBB surface (a), is the zoom of the rectangular area (a1), representative force curves between CNC probe with clean mica surface and the VBB surface (b), (b1) is the zoom of the rectangular area. SEM images of the tip from TOCNF (a2) and CNC probes (b2) after force measurements are shown. The histograms of the distribution of pull off forces of TOCNF functionalised probe with mica (c) and VBB surface (d) and the corresponding average adhesion force value after normalization (e) and the histograms of the distribution of pull off forces of CNC functionalised probes toward mica (f) and VBB surface (g). Corresponding average adhesion force value after normalization (h).

charged character and had the tendency to orient the nitrogens, towards the solvent (Fig. 6 and Fig. S2).

Once VBB was anchored on mica, the direct interaction of VBB with nanocellulose (Fig. 6(a)(b)) was demonstrated by the force curves displayed in Fig. 7(a),(b). The SEM images of the probes after force measurements shown in Fig. 7a2 and b2 indicate that the cellulose nanoparticles remained on the tip, confirming the stability of the probes functionalized by the chemical method.

Compared with the force curves recorded for the interaction between nanocellulose and mica, the separation distance increased from 1 to 3 nm, and a clear snap-in is shown in the approach curve. This indicates that the electrostatic attraction between the negatively charged nanocellulose and positively charged dye dominated the interaction and attracted the tip towards to the surface. However, both double layer and van der Walls attractions could contribute for the snap-in phenomenon.

During retraction, the forces between probes and surfaces are of different nature and include electrostatic, hydrophobic and van der Waals interactions, which could play concertedly important roles in attracting the probe during retraction. The VBB dye has not only a cationic character but also a hydrophobic nature (Steele, Wright, Nygren, & Hillier, 2000). In the case of TOCNF, the average normalized adhesion force increased from 1.3 to 11.0 mN/m (Fig. 7e), indicating a strong electrostatic attraction of the probe to the substrate surface (Fig. 7a1, retract curve). The same mechanism occurred with the CNC system, where the average adhesion force (normalized) increased from 3.7 to 9.2 mN/m (Fig. 7h). The reduced magnitude of the adhesion force for the CNC case is caused by the lower content of functional

groups in relation to TOCNF.

To the best of our knowledge, only a few AFM studies on surface interactions and adhesion force measurements through cellulose based materials were reported in the literature. For example, a pull-off force of around 2–3 nN in dilute salt solutions was first measured between silica and cellulose in the presence of 20 ppm poly[[2-(propionyloxy) ethyl]trimethylammonium chloride] by Holmberg et al in 1997 (Holmberg, Wigren, Erlandsson, & Claesson, 1997). In 2013, the procedure was modified and improved by Saimi et al to measure the adhesion force (in the range of 1–7 mN/m) between a cellulose microsphere and flat cellulose thin film (Olszewska, Valle-Delgado, Nikinmaa, Laine, & Österberg, 2013). Nanocellulose, coated on a spherical carrier, was recently employed to study the adhesion between carbon based materials (1–8 mN/m) (Hajian, Lindström, Pettersson, Hamedi, & Wågberg, 2017) and wood biopolymers (80 mN/m) (Gustafsson et al., 2012). Interaction studies of cellulose based materials with water contaminants were reported only by our group and in 2015 (Shrivastava, 2009) where we disclosed cellulose microspheres surface interactions with Ag(I) ions. In the current work we have greatly improved the method by functionalizing the probes with nanocellulose using chemical method and expanded the application to other metal ions and dyes to derive reliable and quantitative data.

It may be noted that during the force measurements there is the risk that, the copper ions adsorbed on nanocellulose and dye adsorbed on mica may desorb into the aqueous solution, or the positively charged dye molecules might transfer to the negatively charged probe during contact. However, this was prevented by adequately rinsing the system during sample preparation, removing all of the free and loosely attached metal ions and dyes on nanocellulose and mica. All data presented here are based on the assumption that the anchored layers are stable during the measurements.

3.3.4. Molecular dynamics simulations

Starting from random arrangements of the dye molecules in solution relatively close to the supports, migration, adsorption on the interfaces and a marked tendency to self-assemble was observed. The final adsorbed structures were identified through visual inspection and distance evaluations. Also, in this case, RDFs were useful to disclose preferential interactions of the various groups of the molecules in relation to carboxyl and hydroxyl moieties of CNC and TOCNF. The adsorption on all the substrates was confirmed by the presence of sharp peaks at short distances in the RDFs (Fig. 8). The broad peaks reflect the range of nearest-neighbor distances between the selected atoms. The broad trend indicates little inter-atomic ordering, whereas the sharp peaks at short-distances testify the tendency to local coordination, that is hydrogen bonds between N and OH groups or NH and O atoms. Examining the RDF plots of the VBB nitrogen atoms (Fig. 8) it can be noticed that these were hydrogen bonded to the hydroxyl groups of the supports (black peaks centered at around 2.8 Å) both in the CNC and TOCNF models but also solvated by water molecules as demonstrated by in blue plots in Fig. 8 indicating water molecules directly hydrogen bonded to the VBB nitrogens (peaks at 2.8 Å). A second water shell is also visible, is located at about 4.7 Å and solvent exchange between the two shells is active.

Three dimensional iso-surfaces identifying regions most probably occupied by the nitrogen, atoms of the dye (spatial distribution functions - SDFs) during the production simulations are shown in Figs. S3 and S4. The contour density (1.5 times larger than the average solvent density) was chosen in such a way that from those scenarios could emerge a clear picture of the adsorbate behaviour at the cellulose based-material interface and it was visualized on an average configuration calculated from the last portion (100 structures) of the production trajectories. Due to averaging the model can be in some sections unphysical.

The comparison of the SDFs of VBB on CNC and TOCNF (Figs. S3 and S4) indicates that the dye is stably adsorbed on the matrices (N contours located close to the supports) in both cases but seems more mobile when in contact with TOCNF. This could be due to the increased negative charge of the substrate and its redistribution on the interface that perturbs not only the molecular orientation but also the locations of the counterions. Indeed, it is well apparent in the pictures that due to these cooperative effects not only the molecules are driven towards different locations on the surface but also the ions escape far from the support into the solvent (green areas extending into the solvent). Besides lying on the CNC or TOCNF interfaces the dyes can be found in perpendicular arrangements self-interacting by means of their stacked or T-shaped rings. These types of orientation contribute to the formation of molecular aggregates (displayed in Fig. S5) and also agrees well with the findings of VBB aggregates showed in Fig. 6d. Thus, the simulation results well reflect and confirm the discussion of the experimental counterpart.

4. Conclusions

To advance the growing interest to use nanocellulose in water purification as a sustainable technology and to increase the understanding on the adhesion forces and interaction mechanisms between nanocellulose and water pollutants we used colloidal probe technique and molecular dynamics simulation methods. Two representative nanocelluloses with carboxyl surface groups have been successfully functionalized on the sharp AFM probe tips with tip radius below 20 nm by a chemical modification method. In the case of metal ions and dyes the normalized adhesion force was higher for tempo CNF compared to CNC, which was expected due to higher functional group content in the former and in turn confirms the applicability of the nanocellulose functionalized probe for force spectroscopy. The highly promising AFM probes functionalized with nanocellulose could open new possibilities for colloidal probe force spectroscopy technique and could be further employed for recognition imaging and diagnostics (Barattin & Voyer, 2008; Senapati & Lindsay, 2016) in nano and biotechnology.

The interactions with metal ions were further explained by MD simulations, which reproduced the recognition and adsorption mechanism dominated by electrostatic interactions. The simulations identified characteristic arrangements where the molecules of the dyes were aligned perpendicular to the substrates and organized in cluster structures. The surface interactions between the nanocellulose disclosed a flat orientation of the dye on the TOCNF/CNC, adopted to maximize the adsorption and also promote stacking. In the case of metal ions as well as dyes the clustering or aggregation directed by functional sites on nanocellulose was in perfect agreement with the experiments. We aim to extend this approach of employing colloidal probe technique combined with MD simulation to study nanocellulose interactions with other water contaminants (pesticides, drugs, other potentially charged and uncharged entities), foulants (bovine serum albumin, humic acid), bio-species (DNA, protein, blood cells) and polymers (PLA, chitosan) *etc*.

Declaration of Competing Interest

The authors declare no competing financial interest.

Acknowledgements

The authors gratefully acknowledge the financial support of the Swedish research council (VR, grant No: 621-2013-5997 and 2017-04254) and Knut and Alice Wallenberg Foundation under Wallenberg Wood Science Centre (WWSC). We thank Liu, Y. and Naseri, N. who kindly provided the TOCNF and CNC, respectively, from Stockholm University, Sweden. Zhu, C. is especially grateful to Fielden, M. at the Royal Institute of Technology (KTH) Sweden for his technical support and fruitful discussion on force spectroscopy measurements. The Nano lab in AlbaNova university center is also acknowledged for providing

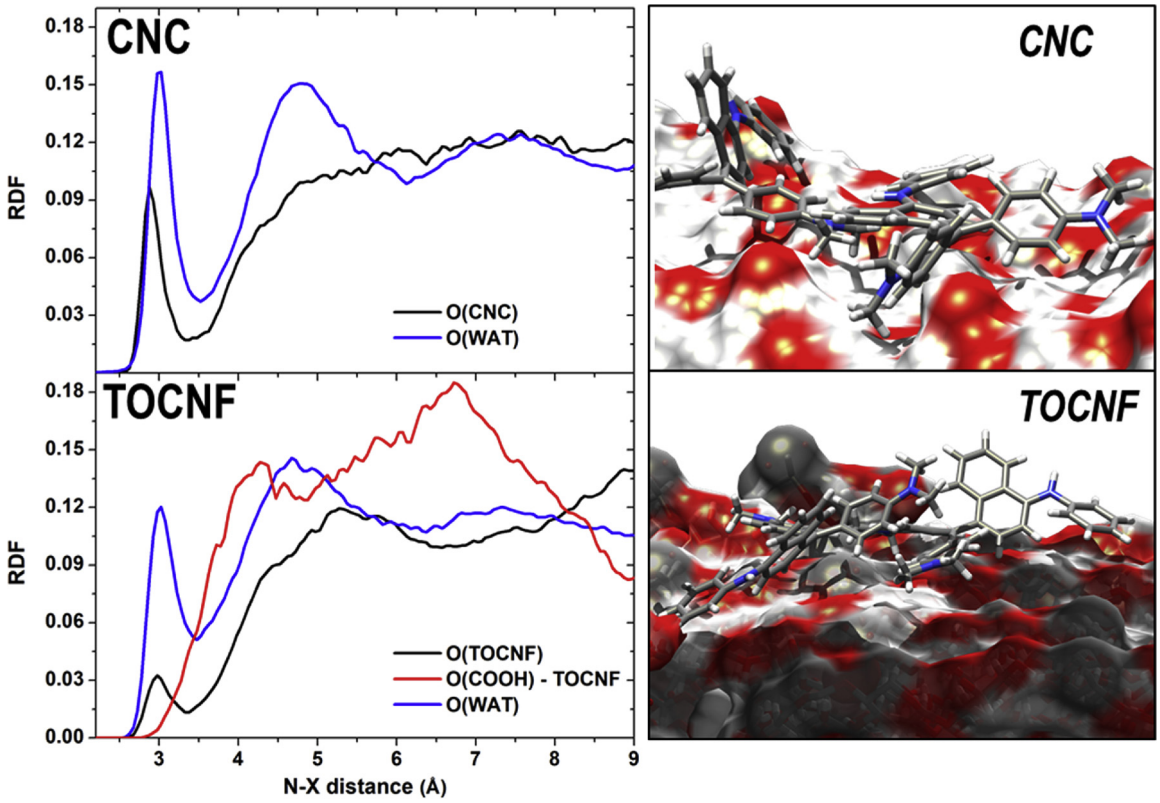

Fig. 8. Left hand side: Normalized RDFs of the adsorption of VBB on the two support types. Only the nitrogen atom of the dye has been considered and its RDFs with all the oxygen types included in the systems have been calculated. Right hand side: Representative configurations where the dyes have maximum interactions with the support lying flat on them. The molecules could be interconnected through stacked or T-shape interactions. VBB are rendered with sticks; nitrogen, oxygen, hydrogen and carbon atoms are blue, red, white and grey, respectively. CNC and TOCNF supports are represented by means of solvent accessible surfaces (solid contours) colored according to the atom type. Water molecules, counterions and portions of CNC and TOCNF substrate have been undisplayed for clarity. (For interpretation of the references to colour in this figure legend, the reader is referred to the web version of this article).

the AFM facilities.

Appendix A. Supplementary data

Supplementary material related to this article can be found, in the online version, at doi:https://doi.org/10.1016/j.carbpol.2019.115510.

References

Abou-Saleh, R. H., Peyman, S. A., Critchley, K., Evans, S. D., & Thomson, N. H. (2013). Nanomechanics of lipid encapsulated microbubbles with functional coatings. *Langmuir, 29*(12).

Alessandrini, A., & Facci, P. (2005). AFM: A versatile tool in biophysics. *Measurement Science & Technology, 16*(6), R65–R92.

Barattin, R., & Voyer, N. (2008). Chemical modifications of AFM tips for the study of molecular recognition events. *Chemical Communications, 13*, 1513–1532.

Beaussart, A., El-Kirat-Chatel, S., Sullan, R. M. A., Alsteens, D., Herman, P., Derclaye, S., et al. (2014). Quantifying the forces guiding microbial cell adhesion using single-cell force spectroscopy. *Nature Protocols, 9*(5), 1049–1055.

Berendsen, H. J. C., Postma, J. P. M., Van Gunsteren, W. F., Dinola, A., & Haak, J. R. (1984). Molecular dynamics with coupling to an external bath. *The Journal of Chemical Physics, 81*(8), 3684–3690.

Chtcheglova, L. A., & Hinterdorfer, P. (2018). Simultaneous AFM topography and recognition imaging at the plasma membrane of mammalian cells. *Seminars in Cell & Developmental Biology, 73*, 45–56.

Corno, M., Delle Piane, M., Monti, S., Moreno-Couranjou, M., Choquet, P., & Ugliengo, P. (2015). Computational study of acidic and basic functionalized crystalline silica surfaces as a model for biomaterial interfaces. *Langmuir, 31*(23), 6321–6331.

Das, P. K., & Bhattacharjee, S. (2005). Electrostatic double layer force between a sphere and a planar substrate in the presence of previously deposited spherical particles. *Langmuir, 21*(10), 4755–4764.

Dhamodharan, R., & McCarthy, T. J. (1999). Adsorption of alginic acid and chondroitin sulfate-A to amine functionality introduced on polychlorotrifluoroethylene and glass surfaces. *Macromolecules, 32*(12), 4106–4112.

Ducker, W. A., Senden, T. J., & Pashley, R. M. (1992). Measurement of forces in liquids using a force microscope. *Langmuir, 8*(7), 1831–1836.

Dufrêne, Y. F. (2017). Microbial nanoscopy: Breakthroughs, challenges, and opportunities. *ACS Nano, 11*(1), 19–22.

Dufrêne, Y. F., Evans, E., Engel, A., Helenius, J., Gaub, H. E., & Müller, D. J. (2011). Five challenges to bringing single-molecule force spectroscopy into living cells. *Nature Methods, 8*, 123–127.

Baerends, E. J., et al. (2016). (n.d.) In E. J. Baerends (Ed.). *106 SCM, theoretical chemistry*. Amsterdam, The Netherlands: Vrije Universiteit.

Ebner, A., Wildling, L., Kamruzzahan, A. S. M., Rankl, C., Wruss, J., Hahn, C. D., et al. (2007). A new, simple method for linking of antibodies to atomic force microscopy tips. *Bioconjugate Chemistry, 18*(4), 1176–1184.

Farquhar, M. L., Vaughan, D. J., Hughes, C. R., Charnock, J. M., & England, K. E. R. (1997). Experimental studies of the interaction of aqueous metal cations with mineral substrates: Lead, cadmium, and copper with perthitic feldspar, muscovite, and biotite. *Geochimica et Cosmochimica Acta, 61*(15), 3051–3064.

Frisbie, C. D., Rozsnyai, L. F., Noy, A., Wrighton, M. S., & Lieber, C. M. (1994). Functional group imaging by chemical force microscopy. *Science, 265*(5181), 2071–2074.

Green, J. B. D., Idowu, A., & Chan, S. S. F. (2003). Modified tips: Molecules to cells. *Materials Today, 6*(2), 22–29.

Groom, C. R., Bruno, I. J., Lightfoot, M. P., & Ward, S. C. (2016). The Cambridge structural database. *Acta Crystallographica Section B, Structural Science, Crystal Engineering and Materials, 72*(2), 171–179.

Gustafsson, E., Johansson, E., Wågberg, L., & Pettersson, T. (2012). Direct adhesive measurements between wood biopolymer model surfaces. *Biomacromolecules, 13*(10), 3046–3053.

Hajian, A., Lindström, S. B., Pettersson, T., Hamedi, M. M., & Wågberg, L. (2017). Understanding the dispersive action of nanocellulose for carbon nanomaterials. *Nano Letters, 17*(3), 1439–1447.

Herman, D., & Walz, J. Y. (2015). Forces and force-scaling in systems of adsorbing nanoparticles as measured using colloidal probe atomic force microscopy. *Colloids and Surfaces A, Physicochemical and Engineering Aspects, 482*, 165–176.

Holmberg, M., Wigren, R., Erlandsson, R., & Claesson, P. M. (1997). Interactions between cellulose and colloidal silica in the presence of polyelectrolytes. *Colloids and Surfaces A, Physicochemical and Engineering Aspects, 129*, 175–183.

Isogai, A., Saito, T., & Fukuzumi, H. (2011). TEMPO-oxidized cellulose nanofibers. *Nanoscale, 3*(1), 71–85.

Kada, G., Kienberger, F., & Hinterdorfer, P. (2008). Atomic force microscopy in bionanotechnology. *Nano Today, 3*(1–2), 12–19.

Kappl, M., & Butt, H.-J. (2002). The colloidal probe technique and its application to adhesion force measurements. *Particle & Particle Systems Characterization, 19*(3),

129–143.
Karim, Z., Mathew, A. P., Grahn, M., Mouzon, J., & Oksman, K. (2014). Nanoporous membranes with cellulose nanocrystals as functional entity in chitosan: Removal of dyes from water. *Carbohydrate Polymers, 112*(0), 668–676.
Kim, M. S., Choi, J. H., Kim, J. H., & Park, Y. K. (2010). Accurate determination of spring constant of atomic force microscope cantilevers and comparison with other methods. *Measurement, 43*(4), 520–526.
Kumar, R., Ramakrishna, S. N., Naik, V. V., Chu, Z., Drew, M. E., Spencer, N. D., et al. (2015). Versatile method for AFM-tip functionalization with biomolecules: Fishing a ligand by means of an in situ click reaction. *Nanoscale, 7*(15), 6599–6606.
Ma, H., Hsiao, B. S., & Chu, B. (2011). Ultrafine cellulose nanofibers as efficient adsorbents for removal of UO22+ in water. *ACS Macro Letters, 1*(1), 213–216.
Mathew, A. P., Oksman, K., Karim, Z., Liu, P., Khan, S. A., & Naseri, N. (2014). Process scale up and characterization of wood cellulose nanocrystals hydrolysed using bioethanol pilot plant. *Industrial Crops and Products, 58*, 212–219.
McNamee, C. E., Pyo, N., & Higashitani, K. (2006). Atomic force microscopy study of the specific adhesion between a colloid particle and a living melanoma cell: Effect of the charge and the hydrophobicity of the particle surface. *Biophysical Journal, 91*(5), 1960–1969.
Möller, R., Csáki, A., Köhler, J. M., & Fritzsche, W. (2000). DNA probes on chip surfaces studied by scanning force microscopy using specific binding of colloidal gold. *Nucleic Acids Research, 28*(20).
Mönig, H., Hermoso, D. R., Arado, O. D., Todorovic, M., Timmer, A., Schüer, S., et al. (2016). Submolecular imaging by noncontact atomic force microscopy with an oxygen atom rigidly connected to a metallic probe. *ACS Nano, 10*(1), 1201–1209.
Monti, S., Alderighi, M., Duce, C., Solaro, R., & Tiné, M. R. (2009). Adsorption of ionic peptides on inorganic supports. *The Journal of Physical Chemistry C, 113*(6), 2433–2442.
Nobile, C., Ashby, P. D., Schuck, P. J., Fiore, A., Mastria, R., Cingolani, R., et al. (2008). Probe tips functionalized with colloidal nanocrystal tetrapods for high-resolution atomic force microscopy imaging. *Small, 4*(12), 2123–2126.
Nugroho, R. W. N., Pettersson, T., Odelius, K., Höglund, A., & Albertsson, A. C. (2013). Force interactions of nonagglomerating polylactide particles obtained through covalent surface grafting with hydrophilic polymers. *Langmuir, 29*(28), 8873–8881.
Olszewska, A., Valle-Delgado, J. J., Nikinmaa, M., Laine, J., & Österberg, M. (2013). Direct measurements of non-ionic attraction and nanoscaled lubrication in biomimetic composites from nanofibrillated cellulose and modified carboxymethylated cellulose. *Nanoscale, 5*(23), 11837–11844.
Pezron, I., Pezron, E., Claesson, P. M., & Malmsten, M. (1991). Temperature-dependent forces between hydrophilic mica surfaces coated with ethyl hydroxyethyl cellulose. *Langmuir, 7*(10), 2248–2252.
Senapati, S., & Lindsay, S. (2016). Recent progress in molecular recognition imaging using atomic force microscopy. *Accounts of Chemical Research, 49*(3), 503–510.
Senapati, S., Manna, S., Lindsay, S., & Zhang, P. (2013). Application of catalyst-free click reactions in attaching affinity molecules to tips of atomic force microscopy for detection of protein biomarkers. *Langmuir, 29*(47), 14622–14630.
Shrivastava, A. K. (2009). A review on copper pollution and its removal from water bodies by pollution control technologies. *Indian Journal of Environmental Protection, 29*(6), 552–560.
Sides, P. J., Faruqui, D., & Gellman, A. J. (2009). Dynamics of charging of muscovite mica: Measurement and modeling. *Langmuir: The ACS Journal of Surfaces and Colloids, 25*(3), 1475–1481.
Steele, H. M., Wright, K., Nygren, M. A., & Hillier, I. H. (2000). Interactions of the (001) surface of muscovite with Cu(II), Zn(II), and Cd(II): A computer simulation study. *Geochimica et Cosmochimica Acta, 64*(2), 257–262.
Valotteau, C., Prystopiuk, V., Pietrocola, G., Rindi, S., Peterle, D., De Filippis, V., et al. (2017). Single-cell and single-molecule analysis unravels the multifunctionality of the staphylococcus aureus collagen-binding protein Cna. *ACS Nano, 11*(2), 2160–2170.
Voisin, H., Bergström, L., Liu, P., & Mathew, A. (2017). Nanocellulose-based materials for water purification. *Nanomaterials, 7*(3), 57–69.
Wada, T., Yamazaki, K., Isono, T., & Ogino, T. (2017). Characterization of local hydrophobicity on sapphire (0001) surfaces in aqueous environment by colloidal probe atomic force microscopy. *Applied Surface Science, 396*, 1206–1211.
Weisenhorn, A. L., Hansma, P. K., Albrecht, T. R., & Quate, C. F. (1989). Forces in atomic force microscopy in air and water. *Applied Physics Letters, 54*(26), 2651–2653.
Wildling, L., Unterauer, B., Zhu, R., Rupprecht, A., Haselgrübler, T., Rankl, C., et al. (2011). Linking of sensor molecules with amino groups to amino-functionalized AFM tips. *Bioconjugate Chemistry, 22*(6), 1239–1248.
Wilson, N. R., & MacPherson, J. V. (2009). Carbon nanotube tips for atomic force microscopy. *Nature Nanotechnology, 4*(8), 483–491.
Wong, S. S., Harper, J. D., Lansbury, P. T., & Lieber, C. M. (1998). Carbon nanotube tips: High-resolution probes for imaging biological systems. *Journal of the American Chemical Society, 120*(3), 603–604.
Zhu, C., Dobryden, I., Rydén, J., Öberg, S., Mathew, A. P., & Holmgren, A. (2015). Adsorption behavior of cellulose and its derivatives toward Ag(I) in aqueous medium: An AFM, spectroscopic, and DFT study. *Langmuir, 31*(45), 12390–12400.
Zhu, C., Liu, P., & Mathew, A. P. (2017). Self-assembled TEMPO cellulose nanofibers: Graphene oxide-based biohybrids for water purification. *ACS Applied Materials & Interfaces, 9*(24), 21048–21058.
Zhu, C., Monti, S., & Mathew, A. P. (2018). Cellulose nanofiber-graphene oxide biohybrids: Disclosing the self-assembly and copper-ion adsorption using advanced microscopy and ReaxFF simulations. *ACS Nano, 12*(7), 7028–7038.
Zhu, H., Fang, Z., Wang, Z., Dai, J., Yao, Y., Shen, F., et al. (2015). Extreme light management in mesoporous wood cellulose paper for optoelectronics. *ACS Nano, 10*(1), 1369–1377.